





Article

Comparative Efficiencies for Phenol Degradation on Solar Heterogeneous Photocatalytic Reactors: Flat Plate and Compound Parabolic Collector

Felipe de J. Silerio-Vázquez ¹, Cynthia M. Núñez-Núñez ², María T. Alarcón-Herrera ^{1,*}
and José B. Proal-Nájera ^{3,*}

¹ Centro de Investigación en Materiales Avanzados, Departamento de Ingeniería Sustentable, S.C. Calle CIMAV 110, Colonia 15 de Mayo, Durango 34147, Mexico; felipe.silerio@cimav.edu.mx

² Ingeniería en Tecnología Ambiental, Universidad Politécnica de Durango, Carretera Durango-México km 9.5, Durango 34300, Mexico; cynthia_cnn@hotmail.com

³ Instituto Politécnico Nacional, CIIDIR-Durango, Calle Sigma 119, Fraccionamiento 20 de Noviembre II, Durango 34220, Mexico

* Correspondence: teresa.alarcon@cimav.edu.mx (M.T.A.-H.); jproal@ipn.mx (J.B.P.-N.); Tel.: +52-614-4394896 (M.T.A.-H.); +52-618-1341781 (J.B.P.-N.)

Abstract: Phenol is a recalcitrant anthropogenic compound whose presence has been reported in both wastewater and drinking water; human exposure to phenolic substances can lead to health problems. The degradation of phenol (measured as COD decrease) through solar heterogeneous photocatalysis with immobilized TiO₂ was performed in two different reactors: a flat-plate reactor (FPR) and a compound parabolic collector (CPC). A 2³ full factorial experimental design was followed. The variables were the presence of TiO₂, H₂O₂ addition, and the type of reactor. Data were fitted to the pseudo-first-order reaction-rate-kinetics model. The rate constant for photocatalytic phenol degradation with 1 mM of H₂O₂ was $6.6 \times 10^{-3} \text{ min}^{-1}$ for the FPR and $5.9 \times 10^{-3} \text{ min}^{-1}$ in the CPC. The calculated figures of merit were analyzed with a MANCOVA, with UV fluence as a covariate. An ANCOVA showed that the type of reactor, H₂O₂ addition, or fluence had no statistically significant effect on the results, but there was for the presence of TiO₂. According to the MANCOVA, fluence and TiO₂ presence were significant ($p < 0.05$). The CPC was on average 17.4% more efficient than the FPR when it came to collector area per order (A_{CO}) by heterogeneous photocatalysis and 1 mM H₂O₂ addition.

Keywords: solar irradiance; titanium dioxide; batch mode; figures of merit; fluence; collector area per order



Citation: Silerio-Vázquez, F.d.J.; Núñez-Núñez, C.M.; Alarcón-Herrera, M.T.; Proal-Nájera, J.B. Comparative Efficiencies for Phenol Degradation on Solar Heterogeneous Photocatalytic Reactors: Flat Plate and Compound Parabolic Collector. *Catalysts* **2022**, *12*, 575. <https://doi.org/10.3390/catal12060575>

Academic Editor: Antonio Eduardo Palomares

Received: 13 April 2022

Accepted: 17 May 2022

Published: 24 May 2022

Publisher's Note: MDPI stays neutral with regard to jurisdictional claims in published maps and institutional affiliations.



Copyright: © 2022 by the authors. Licensee MDPI, Basel, Switzerland. This article is an open access article distributed under the terms and conditions of the Creative Commons Attribution (CC BY) license (<https://creativecommons.org/licenses/by/4.0/>).

1. Introduction

The accelerated industrialization and civilization processes have led to an energy crisis and a state of environmental pollution, which are considered the major threats to the sustainable development of human society [1]. Currently, there is concern regarding the presence of organic compounds in both industrial and municipal wastewater effluents, as they pose a potential threat to the environment (even in trace concentrations); these substances have been categorized as emerging pollutants, and they usually result from the production, use, or disposal of pharmaceuticals, dyes, pesticides, and personal care products, amongst others [2]. It must be remarked that conventional water-treatment technologies have not been designed to remove these substances, hence the development of effective removal strategies has drawn attention [3]. Furthermore, technologies must comply with technical viability, economic feasibility and environmental safety to be considered sustainable [4]. It has been estimated that, worldwide, millions of tons of phenol have been discharged into the environment from industrial waste [5].

Advanced oxidation processes (AOPs), a group of water-treatment technologies, are based on the generation of highly reactive oxygen species (ROS) to degrade organic compounds through oxidation; amongst the AOPs, heterogeneous photocatalysis (HP) has been proposed as a sustainable technology for environmental remediation, including wastewater treatment [6]. HP is based on the use of semiconductors, also known as photocatalysts, whereby light causes an electron from the valence band to migrate to the conduction band, leaving a positive hole (h_{VB}^+) in the valence band, and an extra negative electron (e_{CB}^-) in the conduction band [7]; when in aqueous solution, ROS formation occurs, such as hydroxyl radicals (HO^\bullet), hydrogen peroxide (H_2O_2) and superoxide (O_2^\bullet) [8]. HP can harness solar light and does not need the addition of any other substance [9]; although, adding an appropriate amount of H_2O_2 is a significant strategy to improve photocatalytic activity, as it is an electron scavenger and it undergoes reduction by capturing e_{CB}^- , thereby producing more HO^\bullet [6].

Due to its high reactivity, nontoxicity, high stability, and low cost, nanometric titanium dioxide (TiO_2) is doubtlessly the most researched photocatalyst [10], as the generated ROS along with the h_{VB}^+ could almost decompose any organic compound [11]. Nevertheless, it has its own share of disadvantages, predominantly its limitation to promote HP with only ultraviolet (UV) light, which only comprises 5% of the solar-radiation spectrum [12]. There is a noteworthy scientific interest pertaining to the development of photocatalysts that are active under visible light [13], but this approach does not necessarily imply an activity equal to that of TiO_2 , as the redox reactions fostered by HP are determined by the photocatalyst band positions (valence and conduction band) [14]. TiO_2 use is also prompted by its commercial availability [15].

According to the results reported in the pertinent scientific literature, the technology readiness level for wastewater treatment employing HP is currently between the technological-research and technological-development phases [16]. It is hypothesized that HP system reactivity needs to be enhanced by a factor of 100–1000 in order to be considered at the industrial level [17]. Another challenge is the handling of the photocatalyst; HP is usually performed with the photocatalyst suspended in the media, but due to the photocatalyst size, additional processing is needed to recover it from the treated water, which implies additional costs. This inconvenience can be avoided by immobilizing the photocatalyst with inert material supports, although at the expense of some HP efficiency [18]. So far, the few commercial endeavors, such as Puralytics Lilypad, Puralytics Shield 1000, BrightWater Titanium Advanced Oxidation Process and Purifics PhotoCat, all employ immobilized TiO_2 ; it has thus been deduced that said approach might be the most suitable for technological development to a greater extent [19].

One more difficulty is the relative scarcity of research focused on photocatalytic reactors or systems compared to the research on photocatalytic materials [20,21], which is pertinent to the undeveloped scale-up strategies from the lab to the pilot scale [22]. It has been noted that the design and analysis of a photocatalytic reactor is difficult, as it involves particles of pollutant in a liquid state, the photocatalyst in a solid state, and the phenomena related to light [4]. Photocatalytic reactors have often been designed by empirical endeavors rather than from rigorous scientific principles, as the pertinent engineering knowledge is not extensively available [23].

The lack of design conventions has allowed the presentation of different solar-photocatalytic-reactor designs, such as: slurry fountain, single-baffle, multiple-baffle, solar pond, rectangular chamber with solar concentrator, and offset tubular and cascade; additionally, photocatalytic reactors based on devices for solar-photothermal-energy collection, such as the Fresnel collector, compound parabolic collector (CPC), parabolic through collector or flat-plate reactor (FPR) [20]. It is desirable for solar photocatalytic reactors to: be of low cost, avoid significant temperature increase, be resistant to several weather conditions, make use of both direct and diffuse solar light, have a high optical and photonic efficiency, reduce mass limitations, ensure dissolved oxygen in the medium, be chemically

stable, have a high surface-area-to-volume ratio, and be geometrically appropriate for light propagation and distribution [24].

Low-concentration (one sun) CPC systems have been recommended by many researchers [25], as they are relatively low cost, need no sun-tracking devices, are able to utilize both direct and diffuse solar radiation, are resistant to several weather conditions, and have high optical efficiency [26], as the reflectors allow for an almost entire illumination on tubular reactors [27].

For their part, FPR reactors have high surface-area-to-volume ratio [28], might offer a higher irradiated surface area, and consist of a simple structure [29]; they can also utilize both direct and diffuse sunlight, and since most of the time they are left open to the atmosphere, transmissive losses that might be caused by the cover material and its thickness are eliminated [30].

It is known that the outcome of an HP process depends on diverse factors, i.e., oxygen partial pressure, photocatalyst species, light intensity, light source, pollutant concentration, pH, temperature or reactor geometry; hence, an HP process performed in a reactor, in all likelihood, will differ if performed in another one [4]. Several figures of merit have been proposed to be used as benchmarks for comparison between photocatalytic reactors, such as material-based parameters: reaction rate, reaction rate related to catalyst mass, turnover frequency, turnover number, and space-time yield; additionally, there are the light-based parameters: quantum yield, apparent quantum yield, quantum efficiency, photonic efficiency, photonic yield, power-conversion efficiency, solar-to-chemical-conversion efficiency and photocatalytic space-time yield [31]. Several light-based figures of merit require the solution of the radiative transfer equation, which is a complex and time-consuming task [32,33]; hence, for practical purposes and for solar photocatalytic reactors in the low-concentration regime, the collector area per order proposed by Bolton et al. 2001 [34] is a more accessible figure of merit.

The objective of this paper is to compare the performance of two solar photocatalytic reactors with different geometries: flat plate and compound parabolic collector. The different efficiencies of the reactors were tested by the degradation of phenol (as a model compound, measured through COD) and analyzed through reaction kinetics and statistical tests. Collector area per order (A_{CO}) (m^2/m^3 -order) was also estimated for the evaluation of energy requirements or area required by every reactor.

2. Results and Discussion

2.1. Chemical-Oxygen-Demand Decrease

Figures 1 and 2 show the decrease in chemical-oxygen demand (COD) over time, the former for photolysis (PL) and the latter for HP. The average COD at the beginning of the experiments was 100 ± 6 mg/L.

In all cases, solar PL degradation was exiguous compared to solar HP. Phenol resists solar photodegradation alone to some extent; degradation rates vary between studies, and it can range from small rates that do not reach 10% degradation [35–37] to exemplary rates as high as 38% [38]. It should be noted that solar HP is scarcely reported, and most studies analyze degradation by employing artificial UV light. Invariably, HP degradation surpassed PL degradation in all instances, as rather than relying on UV light alone for degradation, HP ROS generation greatly favored phenol degradation, as the principal ROS generated is HO^\bullet , whose electronegativity is surpassed only by fluorine [39–42].

In the FPR case (Figure 1), PL yielded a slightly higher degradation compared to PL + H_2O_2 , while it performed in contrary fashion in the CPC case. Even though the CPC provides a higher increase in the medium temperature (up to 45 °C), it has been reported that such an increase in temperature plays a negligible role in H_2O_2 decomposition in the absence of photocatalysts [43]; hence, the slight difference in degradation for PL and PL + H_2O_2 in both FPR and CPC is within expectations, as the higher temperature would not foster an increase in HO^\bullet generation.

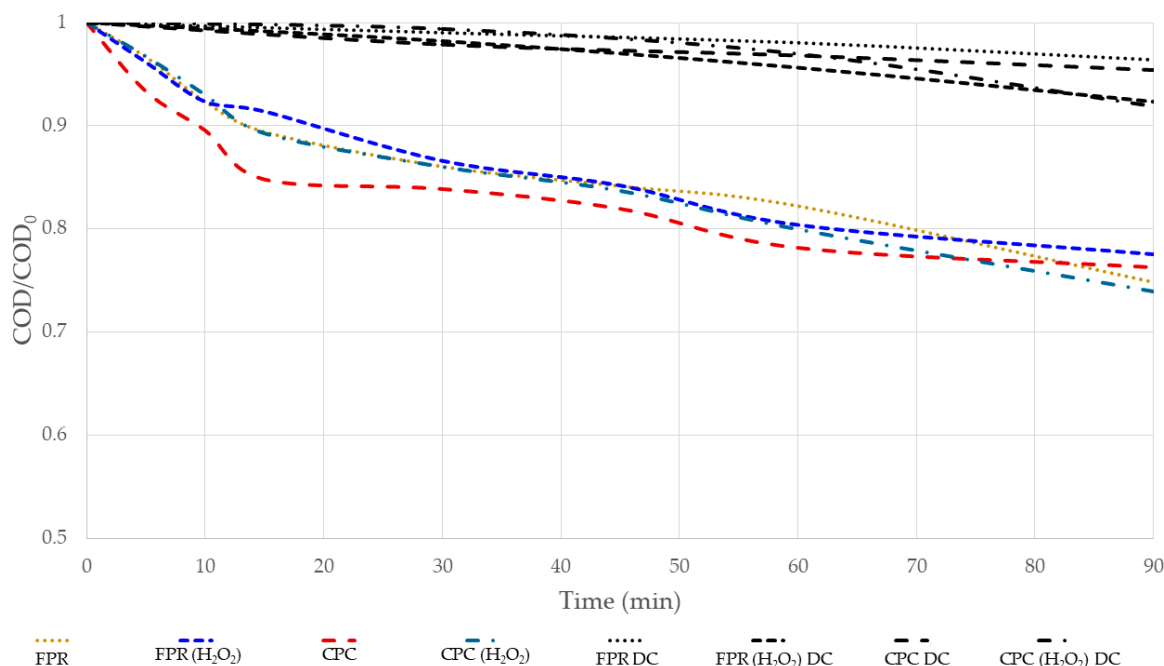


Figure 1. Chemical-oxygen-demand decrease during photolytic degradation for both flat-plate reactor (FPR), with (FPR(H₂O₂)) and without (FPR) H₂O₂ addition, and compound parabolic collector reactor (CPC), with (CPC(H₂O₂)) and without (CPC) H₂O₂ addition. Control experiments performed in the dark (DC) are also included for both flat-plate reactor (FPR), with (FPR (H₂O₂) DC) and without (FPR DC) H₂O₂ addition, and compound parabolic collector reactor (CPC), with (CPC(H₂O₂) DC) and without (CPC DC) H₂O₂ addition.

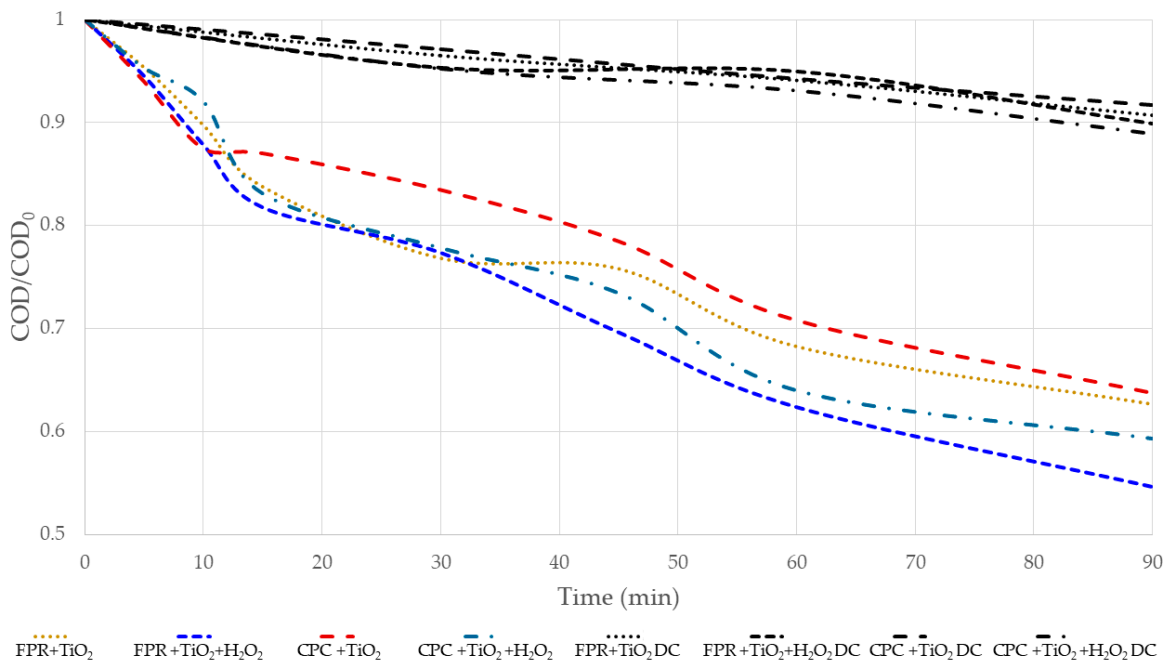


Figure 2. Chemical-oxygen-demand decrease in heterogeneous photocatalytic degradation for both flat-plate reactor (FPR), with (FPR + TiO₂ + H₂O₂) and without (FPR + TiO₂) H₂O₂ addition, and compound parabolic collector reactor (CPC), with (CPC + TiO₂ + H₂O₂) and without (CPC + TiO₂) H₂O₂ addition. Control experiments performed in the dark (DC) are also included for both flat-plate reactor (FPR), with (FPR + TiO₂ + H₂O₂ DC) and without (FPR + TiO₂ DC) H₂O₂ addition, and compound parabolic collector reactor (CPC), with (CPC + TiO₂ + H₂O₂ DC) and without (CPC + TiO₂ DC) H₂O₂ addition.

In HP + H₂O₂ (Figure 2), the degradation was enhanced in both reactors, as H₂O₂ can act as a scavenger for the extra electron in the conduction band, undergo homolytic cleavage, or react with O₂^{-•}, all of which improve HO[•] generation [44]. It has been reported that a high H₂O₂ concentration can negatively impact on the process outcome by decelerating heterogeneous photocatalytic activity [44].

Phenol degradation in control experiments performed in the dark can be considered as negligible when compared with the results obtained in the solar experiments (Figures 1 and 2), as the highest degradation was obtained in HP + H₂O₂ carried out in the CPC (10%) (Figure 2), which can be attributed to adsorption phenomena [45] and oxidation caused by H₂O₂ [46].

In all the experiments, the pH remained between 6.5–7.0; in this range, phenol is mostly found in its molecular form and possesses a neutral charge, while TiO₂ presents a negative surface charge. As the charges are different, an appropriate interfacial contact between TiO₂ and aqueous phenol should occur [47].

2.2. Kinetic Analysis

Table 1 lists the calculated photolytic (k_{ph}) and the photocatalytic (K_{phC}) rate constants for each of the experimental runs. As can be seen, K_{phC} values were higher than those for k_{ph} under the same conditions, and the experiments where a higher COD decrease was observed also showed higher reaction-rate constants.

Table 1. Calculated photolytic and photocatalytic responses to UV reaction-rate constants.

Reactor/H ₂ O ₂	Photolysis (PL)				Heterogeneous Photocatalysis (HP)			
	Photolytic Degradation (%)	Reaction-Rate Constant k_{ph} ($\times 10^{-3} \text{ min}^{-1}$)	Fluence Q_{UV} (kJ/L)	Reaction Rate with Respect to Fluence K_{UV} ($\times 10^{-3} \text{ kJ}^{-1} \text{ L}$)	Photocatalytic Degradation (%)	Reaction-Rate Constant K_{phC} ($\times 10^{-3} \text{ min}^{-1}$)	Fluence Q_{UV} (kJ/L)	Reaction Rate with Respect to Fluence K_{UV} ($\times 10^{-3} \text{ kJ}^{-1} \text{ L}$)
FPR/No H ₂ O ₂	25.2 ± 1.8	2.9	74.6	3.4	37.3 ± 1.5	5.0	71.2	6.4
FPR/1 mM H ₂ O ₂	22.4 ± 1.3	2.7	74.6	3.2	45.4 ± 2.9	6.6	71.2	8.5
CPC/No H ₂ O ₂	23.7 ± 3.3	2.6	105.5	2.2	36.2 ± 1.2	4.6	100.6	4.1
CPC/1 mM H ₂ O ₂	26.1 ± 0.7	3.1	105.5	2.6	40.7 ± 0.5	5.9	100.6	5.2

The coefficient of determination (R^2) for photolytic experiments averaged 0.88, while the photocatalytic experiments averaged 0.93, which can be considered appropriate for fitting the data to the pseudo-first-order-reaction model, which has already been broadly reported to describe phenol degradation via HP [48].

2.3. Fluence Analysis

The fluence (Q_{UV}) for each experimental condition is presented in Table 1 as well. The CPC illuminated area was roughly 40% higher than that of the FPR, which clearly accounts for Q_{UV} being 40% higher in the CPC experiments than in the FPR. However, it is necessary to consider that the photocatalyst-covered area in the CPC was 72% compared to that of the FPR.

The effect of temperature on the outcome of HP has not received enough attention [49] as to propose a plausible hypothesis as of yet. In the past, phenol degradation in heterogeneous photocatalytic processes with TiO₂ was reported to improve as temperature increased. Such improvement was explained by the interfacial rate of electron transfer to oxygen due to an increased recombination rate, the stabilization of the holes located on the oxygen atoms surface due to water adsorption, and an increased pollutant desorption rate, which maintains availability of active sites [50]. Further research is needed on this subject.

The proposed reaction-rate constant in the function of Q_{UV} (K_{UV}) was employed to describe reaction kinetics with respect to cumulative UV dose instead of time [51]; the aver-

aged R^2 values were 0.88 for photolytic experiments, 0.93 for photocatalytic experiments, 0.92 for the FPR and 0.89 for the CPC, compared to 0.88, 0.93, 0.92, and 0.90, which were the R^2 values for the reaction kinetics as a function of time. As the values are almost identical, it can be inferred that reaction kinetics as a function of Q_{UV} can properly explain a reaction, just as reaction kinetics as a function of time.

2.4. Collector Area per Order

Table 2 shows the collector-area-per-order (A_{CO}) value for each of the experimental conditions. The lower the collector area per order, the higher the efficiency of the process. It was found that the CPC needed an average of 28% less photocatalyst area than the FPR. As discussed earlier, one of the effects of adding the reflector to the CPC is to attain more optical efficiency [52], which could account for a better use of the photocatalyst covered area. Nevertheless, offset tubular reactors (without reflectors) have also been reported in the literature [53–56]. An experiment researching the degradation of an organic pollutant compared the performance of an offset tubular reactor with that of a CPC; it concluded that the offset tubular reactor offered the possibility to treat higher volumes, decrease the carbon footprint involved in reactor fabrication, and simplify the reactor scale-up, although at the expense of increasing residence time [57]. Even though the mentioned experiment used a suspended photocatalyst, it poses the question of the actual use of reflectors in photocatalytic reactors.

Table 2. Estimation of A_{CO} , (m^2/m^3 -order) and comparative efficiency for both photolytic and heterogeneous photocatalytic processes, $\epsilon = [(A_{CO_{photol}} - A_{CO_{photocat}}) / (A_{CO_{photol}})] \times 100$, for phenol degradation, based on a first-order reaction ($n = 1$), taking place in a batch mode for FPR and CPC reactors.

Reactor/ H_2O_2	Photolysis Collector Area per Order A_{CO} ($m^2 \cdot m^{-3}$ -Order)	Photocatalysis Collector Area per Order A_{CO} ($m^2 \cdot m^{-3}$ -Order)	Efficiency (ϵ)
FPR/No H_2O_2	111.6	65.2	41.5%
FPR/1 mM H_2O_2	130.2	51.7	60.2%
CPC/No H_2O_2	98.3	50.3	48.7%
CPC/1 mM H_2O_2	77.0	42.7	44.4%

When the comparative efficiencies between both reactors for identical processes was estimated, $\epsilon = [(A_{CO_{FPR}} - A_{CO_{CPC}}) / (A_{CO_{FPR}})] \times 100$, CPC was on average 17.4% more efficient than FPR in terms of collector area per order (A_{CO}) for HP + 1 mM H_2O_2 , 22.8% for HP without added H_2O_2 , 40.8% for photolysis + 1 mM H_2O_2 , and 11.9% for photolysis without H_2O_2 addition.

2.5. ANCOVA and MANCOVA Results

A summary of the analysis-of-covariance (ANCOVA) results is presented in Table 3. The F value for each one of the four ANCOVA linear models were statistically significant ($p < 0.05$), hence we can assume the models were suitable to analyze the experimental design. The models were fitted with R^2 values from 0.78 to 0.92, which means the models can still be improved to yield a better variance explanation [58]. The results support the observations made, as the effect of the PL/HP treatment was statistically significant ($p < 0.05$) on the dependent variables in the four analyses.

H_2O_2 addition did not show a statistically significant effect ($p < 0.05$) in any of the analysis; in a previous work, H_2O_2 showed a statistically significant effect ($p < 0.05$) [47], but the phenol concentration was three times higher than the concentration employed in the present experiment; similarly, the H_2O_2 concentration in the present experiment was 1 mM, while in previous work it was 10 mM; the authors can presuppose that the

proportion of pollutant (phenol, in this particular case) and H₂O₂ has an impact on the outcome of the degradation.

Table 3. Summary of Analysis of Covariance (ANCOVA) for phenol-degradation experiment.

Source	Degrees of Freedom	Sum of Squares ($\times 10^6$)	Mean Square ($\times 10^6$)	F Value	p-Value Probr > F
Degradation (F = 4.03, p = 0.03, R ² = 0.77)					
Reactor	1	338.5	338.5	0.08	0.7
Photocatalyst	1	9.6×10^4	9.6×10^4	22.9	0.001
H ₂ O ₂	1	3.6×10^3	3.6×10^3	0.8	0.3
Reactor*Photocatalyst	1	1.5×10^3	1.5×10^3	0.3	0.5
Reactor*H ₂ O ₂	1	51.5	51.5	0.01	0.9
Photocatalyst*H ₂ O ₂	1	4.2×10^3	4.2×10^3	1.0	0.3
Q _{uv}	1	1.2×10^4	1.2×10^4	2.9	0.1
Reaction Rate (F = 4.64, p = 0.02, R ² = 0.80)					
Reactor	1	0.2	0.2	0.2	0.6
Photocatalyst	1	29.4	29.4	27.1	0.001
H ₂ O ₂	1	2.5	2.5	2.3	0.1
Reactor*Photocatalyst	1	0.3	0.3	0.3	0.5
Reactor*H ₂ O ₂	1	0.02	0.02	0.02	0.8
Photocatalyst*H ₂ O ₂	1	1.5	1.5	1.4	0.2
Q _{uv}	1	1.1	1.1	1.0	0.3
Reaction Rate (Q _{uv}) (F = 5.02, p = 0.01, R ² = 0.81)					
Reactor	1	7.5	0.02	7.5	0.02
Photocatalyst	1	22.8	0.001	22.8	0.001
H ₂ O ₂	1	1.6	0.2	1.6	0.2
Reactor*Photocatalyst	1	1.8	0.2	1.8	0.2
Reactor*H ₂ O ₂	1	0.01	0.9	0.01	0.9
Photocatalyst*H ₂ O ₂	1	1.2	0.3	1.2	0.3
Q _{uv}	1	0.0	0.9	0.0	0.9
Collector area per order (F = 13.1, p = 0.0008, R ² = 0.92)					
Reactor	1	9.4×10^8	9.4×10^8	7.5	0.02
Photocatalyst	1	9.7×10^9	9.7×10^9	78.6	<0.0001
H ₂ O ₂	1	2.3×10^8	2.3×10^8	1.8	0.2
Reactor*Photocatalyst	1	2.5×10^8	2.5×10^8	2.0	0.1
Reactor*H ₂ O ₂	1	1.3×10^8	1.3×10^8	1.1	0.3
Photocatalyst*H ₂ O ₂	1	3.1×10^7	3.1×10^7	0.2	0.6
Q _{uv}	1	6.0×10^7	6.0×10^7	0.4	0.5

Additionally relevant, the type of reactor had no statistically significant effect ($p < 0.05$) on the degradation or reaction rate, but it did effect the A_{CO} and K_{UV} , which is expected, as it has been reported that the reactor geometry is critical in heterogeneous photocatalytic processes [59]. It can be assumed that the employed figure of merit is relevant for the analysis, and further figures of merit might be proposed in order to understand the phenomena better, such as the photocatalytic space-time yield or superficial area to volume ratio [21].

None of the two variable interactions showed a statistically significant effect ($p < 0.05$), so it can be inferred that there is no synergy between the analyzed variables. Q_{UV} was not statistically significant either ($p < 0.05$), which can be attributed to the consistency of the experimental conditions (operation during solar noon, on sunny days and over a relatively short period) [47].

The multivariate-analysis-of-covariance (MANCOVA) results are shown in Table 4. The Roy's greatest root value was used to evaluate whether each of the independent variables and their interactions had an overall effect on the dependent variables. Most of the results support the ANCOVA findings, as it is shown that the presence of TiO_2 was significant; nevertheless, its interaction with the type of reactor was significant as well, which is in discrepancy with the ANCOVA. More notably, Q_{UV} was also significant ($p < 0.05$), which indicates the model can still be improved.

Table 4. Summary of No Overall Effect Multivariate Analysis of Covariance (MANCOVA) for phenol-degradation experiment.

Source	Roy's Greatest Root Value	F Value	Numerator Degrees of Freedom	Denominator Degrees of Freedom	Pr > F
Reactor	2.6	3.3	4	5	0.11
Photocatalyst	13.8	17.2	4	5	0.003
H_2O_2	2.4	3.0	4	5	0.12
Reactor*Photocatalyst	7.2	9.0	4	5	0.01
Reactor* H_2O_2	0.8	1.0	4	5	0.45
Photocatalyst* H_2O_2	0.3	0.3	4	5	0.80
Q_{uv}	7.4	9.2	4	5	0.01

These findings are valuable, as experiments comparing reactors are scarce; additionally, it has been considered that the reactors differ in several operational and physical parameters, which sheds light on the fact that several of the aforementioned variables (oxygen partial pressure, photocatalyst species, light intensity, light source, pollutant concentration, pH, temperature, reactor geometry) really do affect the outcome of a heterogeneous photocatalytic process, which deserves further research.

3. Materials and Methods

3.1. Experimental Phase Location and Operation Timeframe

The experimental phase took place in the city of Durango (25.61° N, 103.43° W, 1900 m above sea level; Durango, Mexico). Experiments were carried out in late July, in the summer season, for 90 min during solar noon. Typically, average solar radiation surpasses 900 W/m² [47].

3.2. Photocatalytic Reactors

Phenol degradation was carried out in two different solar photocatalytic reactors: an inclined flat-plate reactor (FPR) and a compound-parabolic-collector reactor (CPC) (Figure 3). The FPR consisted of a chamber made of polymethylmethacrylate (PMMA) supported by a reclining metal structure. The chamber was equipped at the top with a polyvinyl chloride feeding pipe with small holes every 0.5 cm and, at the chamber's bottom, a drainage that led to a reservoir for the fluid. The sample was recirculated throughout the reactor using a submersible water pump (Model H-331 BioPro, Jiangsu, China).

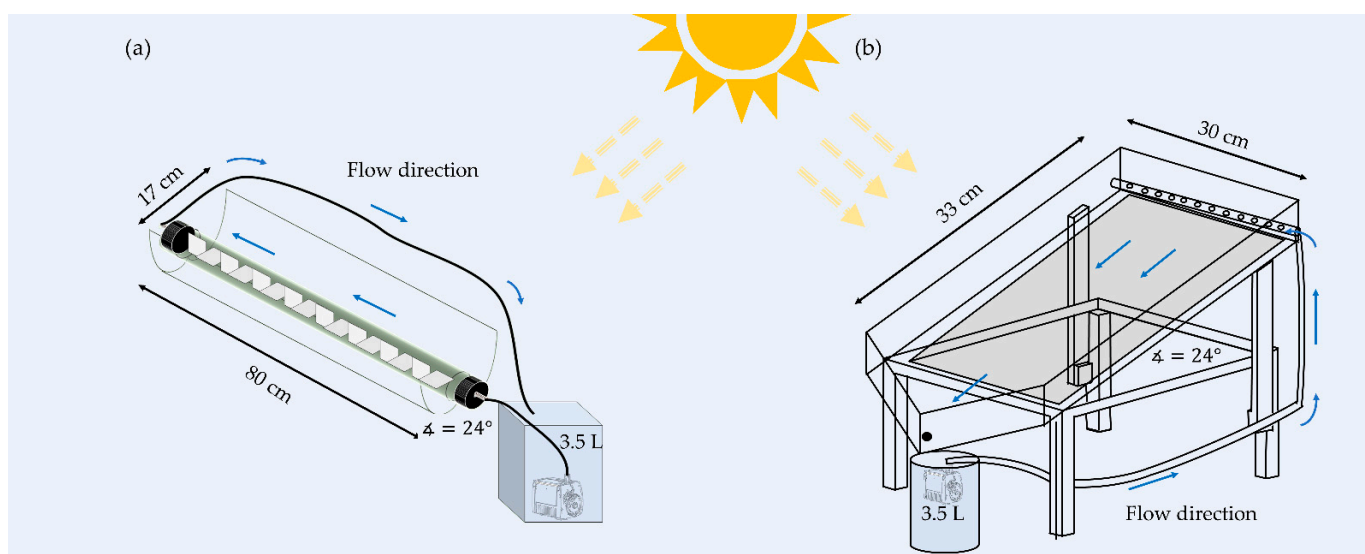


Figure 3. Experimental setup and reactor schematics: (a) CPC reactor (b) FPR reactor.

The CPC reactor consisted of a 3 mm-thick PMMA tube, with 3 mm-thick PMMA plates placed inside. The sample was fed into one end of the tube from a fluid reservoir using a submersible water pump; the other end connected to a hose that delivered the fluid back to the container. The tube was placed on a homemade compound parabolic reflector made of a galvanized iron sheet covered with commercial reflective adhesive paper.

In the FPR, TiO₂ was immobilized on a 30 cm-length and 33 cm-width frosted-glass plate. On the CPC, it was immobilized on sixteen 5 cm-length and 4.5 cm-width PMMA plates (both sides of the plate). A combination of previously reported methodologies was used [60,61]: plates were pre-heated at 100 °C for 10 min; then, 10 mL of a suspension containing TiO₂ (Degussa-Evonik, CAS: 13463-67-7, Germany) were sprayed onto the plates employing a commercial air brush and an air compressor; the TiO₂-sprayed plates were dried at 100 °C for 10 min [47]. TiO₂ was immobilized onto the support surfaces at a ratio of 2 g/m² [62].

Two reactors of each geometry were available to perform duplicate experiments; reactors were tilted at 24° inclination [63], facing south, which corresponds to an azimuthal angle of 180°, in order to maximize solar irradiance orthogonal incidence (with respect to a flat surface) [64]. Table 5 shows the operational parameters, which differed for each reactor. Figure 3 depicts the experimental setup.

Table 5. Different operational parameters between reactors.

Reactor	Illuminated Net Area (m ²)	Photocatalyst Covered Area (m ²)	Volumetric Flow (m ³ /h)
FPR	0.10 ¹	0.10 ¹	0.18
CPC	1.40 ²	0.07 ³	1.50

¹ Glass plate area, equal to the photocatalyst covered area; ² Reactor parabolic reflector area; ³ PMMA plates photocatalyst covered area.

3.3. Experimental Conditions

A total of 3.5 L of a 100 mg/L phenol (Sigma-Aldrich, Schnellendorf, Germany. CAS: 108-95-2) solution prepared with deionized water was employed for each experimental run, which lasted for 90 min (beginning 45 min before solar noon); 2 mL samples were taken during the experiment (at 0, 5, 10, 15, 30, 45, 60 and 90 min) in order to quantify COD. For the experiments making use of H₂O₂, 0.358 mL from a 30% H₂O₂ (Fermont, Guadalajara, Mexico. CAS: 7722-84-1) stock solution was added to the phenol solution, in order to achieve

H₂O₂ 1 mM concentration. UV solar radiation was measured throughout the experiment by employing a radiometer (CUV5, Kipp & Zonen, Delft, The Netherlands). Control experiments performed in the dark were carried out for each of the experimental conditions.

3.4. Chemical Oxygen Demand Quantification

COD was quantified by the Method 8000 from the Hach Handbook of Water Analysis, which is approved by the USEPA under 40 CFR 136.3 [65]. COD TNTplus HR vial tests, a digital reactor block DRB200 and a DR-6000 spectrophotometer, all provided by Hach (Loveland, CO, USA), were used. COD quantification is an appropriate analysis to evaluate the extent of the complete degradation of an organic pollutant [47,66].

3.5. Kinetic Analysis

It has been reported that the photocatalytic degradation of phenolic pollutants can be fitted to the pseudo-first-order rate equation, which is often observed in TiO₂ photocatalysis, and is attributed to a constant generation of reactive species under stable conditions [67,68].

COD data were used to determine the K_{phC} , or the k_{ph} , which were obtained by fitting the data to the pseudo-first-order-reaction model.

For the photolytic experiments, the pseudo-first-order equation was determined by well-known formal kinetics [69], considered as shown in Equation (1):

$$[\text{COD}]_t = [\text{COD}]_0 e^{-k_{\text{ph}} t} \quad (1)$$

where $[\text{COD}]_0$ is the COD at $t = 0$, and $[\text{COD}]_t$ is the COD at the time t ; laminar flow within the reactor ($Re < 1000$), constant fluid density and viscosity, and steady-state operation were considered as assumptions [70].

K_{phC} was determined employing Equation (2) [66,71,72]:

$$[\text{COD}]_t = [\text{COD}]_0 e^{-K_{\text{phC}} t} \quad (2)$$

where K_{phC} is the photocatalytic reaction-rate constant.

3.6. Fluence Analysis

To calculate Q_{UV} , the protocol proposed by [51,73–75] was used. Q_{UV} with respect to the time was calculated as indicated in Equation (3):

$$Q_{\text{UV}} = Q_{\text{UV},n-1} + UV_n \cdot (t_n - t_{n-1}) \cdot \frac{A_i}{V_t}, \quad (3)$$

where Q_{UV} is the fluence, UV_n is the UV irradiance, t_n is the time, A_i is the net irradiated area and V_t is the total volume. According to [51], we can calculate $[\text{COD}]_t$ as a function of Q_{UV} by Equation (4):

$$[\text{COD}]_t = [\text{COD}]_0 e^{-K_{\text{UV}} Q_{\text{UV}}}, \quad (4)$$

where K_{UV} represents the rate constant calculated under fluence Q_{UV} .

3.7. Collector Area per Order Determination

Employing the reaction-kinetics order obtained, the collector area per order was calculated as described by Bolton et al., 2001 [34]; by Equation (5):

$$A_{\text{CO}} = \frac{A_c \bar{E}_s t}{V_t \log\left([\text{COD}]_0 / [\text{COD}]_f\right)} \quad (5)$$

Collector area per order (A_{CO}) is defined as the area of irradiated photocatalyst needed (A_c) to reduce the concentration of a pollutant ($[\text{COD}]$) in a unit of volume (V_t) by one order of magnitude in a given time (t), considering an average UV solar irradiance (\bar{E}_s) [34,62].

3.8. Experimental Design

A full factorial 2^3 experimental design was employed to test the effects of the type of reactor, and control experiments without TiO_2 and experiments with H_2O_2 addition were also performed, completing two levels for each variable. MANCOVA and ANOVA were used to determine if the effect of the independent variables was significant in the outcome of the dependent variables [76]. The linear model employed was as Equation (6) describes:

$$\begin{matrix} w_{ijk} \\ x_{ijk} \\ y_{ijk} \\ z_{ijk} \end{matrix} = \bar{\mu} + P_i + R_j + H_k + \alpha C + \varepsilon_{ijk}, \quad (6)$$

where, w_{ijk} , x_{ijk} , y_{ijk} and z_{ijk} represent phenol degradation, reaction-rate constant, reaction-rate constant as a function of fluence, and collector area per order, respectively; $\bar{\mu}$ is the general mean, P_i represents the presence of photocatalyst, R_j represents the reactor type, H_k represents addition of H_2O_2 , α stands for the regression coefficient of the covariate, C is the covariate (Q_{UV}) and ε represents the lineal model error. The statistical software SAS Studio 3.8 (SAS Institute Inc., Cary, NC, USA) was used to carry out the analysis.

4. Conclusions

It was found that HP with 1 mM H_2O_2 yielded the best performance for phenol degradation, reaching 45.4% for the FPR and 40.7% for the CPC.

The COD decrease fitted well with the pseudo-first-order rate equation, and the proposed K_{UV} showed a higher R^2 . K_{pHC} for phenol degradation with 1 mM of H_2O_2 was $6.6 \times 10^{-3} \text{ min}^{-1}$ for the FPR, while it was $5.9 \times 10^{-3} \text{ min}^{-1}$ in the CPC.

The ANCOVA analysis showed there was no statistically significant effect on the outcome of the reaction when it was carried out in any of the two reactor designs, despite some differences in operational parameters, which merit further research. Q_{UV} did not show a significant effect in the ANCOVA on any of the dependent variables, but the MANCOVA did show a significant overall effect, which indicates the model can be further improved.

The type of reactor had no statistically significant effect ($p < 0.05$) on the degradation or reaction rate, but it did on the A_{CO} and K_{UV} . The CPC was on average 17.4% more efficient than the FPR when it came to collector area per order (A_{CO}) for HP + 1 mM H_2O_2 , 22.8% for HP without H_2O_2 addition, 40.8% for PL + 1 mM H_2O_2 , and 11.9% for PL without H_2O_2 addition.

Author Contributions: Conceptualization, F.d.J.S.-V. and J.B.P.-N.; Data curation, F.d.J.S.-V.; Formal analysis, F.d.J.S.-V. and C.M.N.-N.; Investigation, F.d.J.S.-V.; Methodology, F.d.J.S.-V. and J.B.P.-N.; Resources, M.T.A.-H. and J.B.P.-N.; Supervision, M.T.A.-H. and J.B.P.-N.; Visualization, C.M.N.-N., M.T.A.-H. and J.B.P.-N.; Writing—original draft, F.d.J.S.-V.; Writing—review & editing, C.M.N.-N., M.T.A.-H. and J.B.P.-N. All authors have read and agreed to the published version of the manuscript.

Funding: The research was internally financed by Centro de Investigación en Materiales Avanzados and Instituto Politécnico Nacional SIP:20210507 and SIP:20220741. First author received a scholarship provided by Consejo Nacional de Ciencia y Tecnología.

Institutional Review Board Statement: Not applicable.

Informed Consent Statement: Not applicable.

Data Availability Statement: All data and materials have been provided within the manuscript.

Acknowledgments: The authors would like to thank AMD Planta de Tratamiento de Aguas Residuales "Oriente" of Durango, Mexico, for allowing the use of its installations for the experimental phase.

Conflicts of Interest: The authors declare no conflict of interest to disclose. Funders played no role in study design; data collection, analysis, and interpretation; manuscript writing; results publication.

References

1. Qian, Y.; Ma, D. Covalent Organic Frameworks: New Materials Platform for Photocatalytic Degradation of Aqueous Pollutants. *Materials* **2021**, *14*, 5600. [[CrossRef](#)] [[PubMed](#)]
2. Rueda-Marquez, J.J.; Levchuk, I.; Fernández Ibañez, P.; Sillanpää, M. A critical review on application of photocatalysis for toxicity reduction of real wastewaters. *J. Clean. Prod.* **2020**, *258*, 120694. [[CrossRef](#)]
3. Liang, Y.; Huang, G.; Xin, X.; Yao, Y.; Li, Y.; Yin, J.; Li, X.; Wu, Y.; Gao, S. Black titanium dioxide nanomaterials for photocatalytic removal of pollutants: A review. *J. Mater. Sci. Technol.* **2022**, *112*, 239–262. [[CrossRef](#)]
4. Sundar, K.P.; Kanmani, S. Progression of Photocatalytic reactors and it's comparison: A Review. *Chem. Eng. Res. Des.* **2020**, *154*, 135–150. [[CrossRef](#)]
5. Mohamad Said, K.A.; Ismail, A.F.; Abdul Karim, Z.; Abdullah, M.S.; Hafeez, A. A review of technologies for the phenolic compounds recovery and phenol removal from wastewater. *Process Saf. Environ. Prot.* **2021**, *151*, 257–289. [[CrossRef](#)]
6. Wang, H.; Li, X.; Zhao, X.; Li, C.; Song, X.; Zhang, P.; Huo, P.; Li, X. A review on heterogeneous photocatalysis for environmental remediation: From semiconductors to modification strategies. *Chin. J. Catal.* **2022**, *43*, 178–214. [[CrossRef](#)]
7. Ma, D.; Liu, A.; Li, S.; Lu, C.; Chen, C. TiO₂ photocatalysis for C–C bond formation. *Catal. Sci. Technol.* **2018**, *8*, 2030–2045. [[CrossRef](#)]
8. Wang, W.; Tadó, M.O.; Shao, Z. Nitrogen-doped simple and complex oxides for photocatalysis: A review. *Prog. Mater. Sci.* **2018**, *92*, 33–63. [[CrossRef](#)]
9. Colmenares, J.C. Selective redox photocatalysis: Is there any chance for solar bio-refineries? *Curr. Opin. Green Sustain. Chem.* **2019**, *15*, 38–46. [[CrossRef](#)]
10. Zhang, Y.; Hawboldt, K.; Zhang, L.; Lu, J.; Chang, L.; Dwyer, A. Carbonaceous nanomaterial-TiO₂ heterojunctions for visible-light-driven photocatalytic degradation of aqueous organic pollutants. *Appl. Catal. A Gen.* **2022**, *630*, 118460. [[CrossRef](#)]
11. Ma, D.; Li, J.; Liu, A.; Chen, C. Carbon Gels-Modified TiO₂: Promising Materials for Photocatalysis Applications. *Materials* **2020**, *13*, 1734. [[CrossRef](#)] [[PubMed](#)]
12. Jiang, L.; Yang, J.; Zhou, S.; Yu, H.; Liang, J.; Chu, W.; Li, H.; Wang, H.; Wu, Z.; Yuan, X. Strategies to extend near-infrared light harvest of polymer carbon nitride photocatalysts. *Coord. Chem. Rev.* **2021**, *439*, 213947. [[CrossRef](#)]
13. González-González, R.B.; Parra-Arroyo, L.; Parra-Saldívar, R.; Ramirez-Mendoza, R.A.; Iqbal, H.M.N. Nanomaterial-based catalysts for the degradation of endocrine-disrupting chemicals—A way forward to environmental remediation. *Mater. Lett.* **2022**, *308*, 131217. [[CrossRef](#)]
14. Shaham-Waldmann, N.; Paz, Y. Away from TiO₂: A critical minireview on the developing of new photocatalysts for degradation of contaminants in water. *Mater. Sci. Semicond. Process.* **2016**, *42*, 72–80. [[CrossRef](#)]
15. Tawfik, A.; Alalm, M.G.; Awad, H.M.; Islam, M.; Qyyum, M.A.; Al-Muhtaseb, A.H.; Osman, A.I.; Lee, M. Solar photo-oxidation of recalcitrant industrial wastewater: A review. *Environ. Chem. Lett.* **2022**, *20*, 1839–1862. [[CrossRef](#)]
16. Iervolino, G.; Zammit, I.; Vaiano, V.; Rizzo, L. Limitations and Prospects for Wastewater Treatment by UV and Visible-Light-Active Heterogeneous Photocatalysis: A Critical Review. *Top. Curr. Chem.* **2020**, *378*, 7. [[CrossRef](#)]
17. da Costa Filho, B.M.; Vilar, V.J.P. Strategies for the intensification of photocatalytic oxidation processes towards air streams decontamination: A review. *Chem. Eng. J.* **2019**, *391*, 123531. [[CrossRef](#)]
18. Karavasilis, M.V.; Theodoropoulou, M.A.; Tsakiroglou, C.D. Photocatalytic Degradation of Dissolved Phenol by Immobilized Zinc Oxide Nanoparticles: Batch Studies, Continuous Flow Experiments, and Numerical Modeling. *Nanomaterials* **2021**, *12*, 69. [[CrossRef](#)]
19. Dossin Zanrosso, C.; Piazza, D.; Lansarin, M.A. Solution mixing preparation of PVDF/ZnO polymeric composite films engineered for heterogeneous photocatalysis. *J. Appl. Polym. Sci.* **2020**, *137*, 48417. [[CrossRef](#)]
20. Silerio-Vázquez, F.; Proal Nájera, J.B.; Bundschuh, J.; Alarcon-Herrera, M.T. Photocatalysis for arsenic removal from water: Considerations for solar photocatalytic reactors. *Environ. Sci. Pollut. Res.* **2021**. [[CrossRef](#)]
21. Leblebici, M.E.; Stefanidis, G.D.; Van Gerven, T. Comparison of photocatalytic space-time yields of 12 reactor designs for wastewater treatment. *Chem. Eng. Process. Process Intensif.* **2015**, *97*, 106–111. [[CrossRef](#)]
22. Verma, A.; Tejo Prakash, N.; Toor, A.P.; Bansal, P.; Sangal, V.K.; Kumar, A. Concentrating and Nonconcentrating Slurry and Fixed-Bed Solar Reactors for the Degradation of Herbicide Isoproturon. *J. Sol. Energy Eng.* **2018**, *140*, 021006. [[CrossRef](#)]
23. Colina-Márquez, J.; Machuca-Martínez, F.; Puma, G.L. Radiation Absorption and Optimization of Solar Photocatalytic Reactors for Environmental Applications. *Environ. Sci. Technol.* **2010**, *44*, 5112–5120. [[CrossRef](#)]
24. Abdel-Maksoud, Y.K.; Imam, E.; Ramadan, A.R. TiO₂ water-bell photoreactor for wastewater treatment. *Sol. Energy* **2018**, *170*, 323–335. [[CrossRef](#)]
25. Malinowski, S.; Presečki, I.; Jajčinović, I.; Brnardić, I.; Mandić, V.; Grčić, I. Intensification of Dihydroxybenzenes Degradation over Immobilized TiO₂ Based Photocatalysts under Simulated Solar Light. *Appl. Sci.* **2020**, *10*, 7571. [[CrossRef](#)]
26. Talwar, S.; Verma, A.K.; Sangal, V.K.; Štangar, U.L. Once through continuous flow removal of metronidazole by dual effect of photo-Fenton and photocatalysis in a compound parabolic concentrator at pilot plant scale. *Chem. Eng. J.* **2020**, *388*, 124184. [[CrossRef](#)]
27. Martínez-Costa, J.I.; Maldonado Rubio, M.I.; Leyva-Ramos, R. Degradation of emerging contaminants diclofenac, sulfamethoxazole, trimethoprim and carbamazepine by bentonite and vermiculite at a pilot solar compound parabolic collector. *Catal. Today* **2020**, *341*, 26–36. [[CrossRef](#)]

28. Hama Aziz, K.H.; Miessner, H.; Mueller, S.; Mahyar, A.; Kalass, D.; Moeller, D.; Khorshid, I.; Rashid, M.A.M. Comparative study on 2,4-dichlorophenoxyacetic acid and 2,4-dichlorophenol removal from aqueous solutions via ozonation, photocatalysis and non-thermal plasma using a planar falling film reactor. *J. Hazard. Mater.* **2018**, *343*, 107–115. [[CrossRef](#)]
29. Constantino, D.S.M.; Dias, M.M.; Silva, A.M.T.; Faria, J.L.; Silva, C.G. Intensification strategies for improving the performance of photocatalytic processes: A review. *J. Clean. Prod.* **2022**, *340*, 130800. [[CrossRef](#)]
30. Lou, W.; Kane, A.; Wolbert, D.; Rtimi, S.; Assadi, A.A. Study of a photocatalytic process for removal of antibiotics from wastewater in a falling film photoreactor: Scavenger study and process intensification feasibility. *Chem. Eng. Process. Process Intensif.* **2017**, *122*, 213–221. [[CrossRef](#)]
31. Welter, E.S.; Kött, S.; Brandenburg, F.; Krömer, J.; Goepel, M.; Schmid, A.; Gläser, R. Figures of merit for photocatalysis: Comparison of NiO/La-NaTaO₃ and *Synechocystis* sp. pcc 6803 as a semiconductor and a bio-photocatalyst for water splitting. *Catalysts* **2021**, *11*, 1415. [[CrossRef](#)]
32. Camera-Roda, G.; Augugliaro, V.; Cardillo, A.G.; Loddo, V.; Palmisano, L.; Parrino, F.; Santarelli, F. A reaction engineering approach to kinetic analysis of photocatalytic reactions in slurry systems. *Catal. Today* **2016**, *259*, 87–96. [[CrossRef](#)]
33. Brucato, A.; Cassano, A.E.; Grisafi, F.; Montante, G.; Rizzuti, L.; Vella, G. Estimating Radiant Fields in Flat Heterogeneous Photoreactors by the Six-Flux Model. *AIChE J.* **2006**, *52*, 3882–3890. [[CrossRef](#)]
34. Bolton, J.R.; Bircher, K.G.; Tumas, W.; Tolman, C.A. Figures-of-merit for the technical development and application of advanced oxidation technologies for both electric- and solar-driven systems (IUPAC Technical Report). *Pure Appl. Chem.* **2001**, *73*, 627–637. [[CrossRef](#)]
35. Mohamed, A.; Yousef, S.; Nasser, W.S.; Osman, T.A.; Knebel, A.; Sánchez, E.P.V.; Hashem, T. Rapid photocatalytic degradation of phenol from water using composite nanofibers under UV. *Environ. Sci. Eur.* **2020**, *32*, 160. [[CrossRef](#)]
36. Bali, U.; Çatalkaya, E.Ç.; Şengül, F. Photochemical Degradation and Mineralization of Phenol: A Comparative Study. *J. Environ. Sci. Heal. Part A* **2003**, *38*, 2259–2275. [[CrossRef](#)]
37. Vilhunen, S.; Puton, J.; Virkutyte, J.; Sillanpää, M. Efficiency of hydroxyl radical formation and phenol decomposition using UV light emitting diodes and H₂O₂. *Environ. Technol.* **2011**, *32*, 865–872. [[CrossRef](#)]
38. Nguyen, A.T.; Juang, R.S. Photocatalytic degradation of p-chlorophenol by hybrid H₂O₂ and TiO₂ in aqueous suspensions under UV irradiation. *J. Environ. Manag.* **2015**, *147*, 271–277. [[CrossRef](#)]
39. Kanakaraju, D.; Glass, B.D.; Oelgemöller, M. Advanced oxidation process-mediated removal of pharmaceuticals from water: A review. *J. Environ. Manag.* **2018**, *219*, 189–207. [[CrossRef](#)]
40. Alrousan, D.M.A.; Dunlop, P.S.M.; McMurray, T.A.; Byrne, J.A. Photocatalytic inactivation of *E. coli* in surface water using immobilised nanoparticle TiO₂ films. *Water Res.* **2009**, *43*, 47–54. [[CrossRef](#)]
41. Ola, O.; Maroto-Valer, M.M. Review of material design and reactor engineering on TiO₂ photocatalysis for CO₂ reduction. *J. Photochem. Photobiol. C Photochem. Rev.* **2015**, *24*, 16–42. [[CrossRef](#)]
42. Eskandarian, M.R.; Choi, H.; Fazli, M.; Rasoulifard, M.H. Effect of UV-LED wavelengths on direct photolytic and TiO₂ photocatalytic degradation of emerging contaminants in water. *Chem. Eng. J.* **2016**, *300*, 414–422. [[CrossRef](#)]
43. Naghmash, M.A.; Saif, M.; Mahmoud, H.R. Transition metal ions doped Bi₁₂SiO₂₀ as novel catalysts for the decomposition of hydrogen peroxide (H₂O₂). *J. Taiwan Inst. Chem. Eng.* **2021**, *121*, 268–275. [[CrossRef](#)]
44. Adishkumar, S.; Kanmani, S. Treatment of phenolic wastewaters in single baffle reactor by solar/TiO₂/H₂O₂ process. *Desalin. Water Treat.* **2010**, *24*, 67–73. [[CrossRef](#)]
45. Bekkouche, S.; Bouhelassa, M.; Salah, N.H.; Meghlaoui, F.Z. Study of adsorption of phenol on titanium oxide (TiO₂). *Desalination* **2004**, *166*, 355–362. [[CrossRef](#)]
46. Maurya, M.R.; Titinchi, S.J.J.; Chand, S. Oxidation of phenol with H₂O₂ catalysed by Cu(II), Ni(II) and Zn(II) complexes of *N,N'*-bis-(salicylidene)diethylenetriamine (H₂saldien) encapsulated in Y-zeolite. *J. Mol. Catal. A Chem.* **2003**, *201*, 119–130. [[CrossRef](#)]
47. Silerio-Vázquez, F.; Alarcón-Herrera, M.T.; Proal-Nájera, J.B. Solar heterogeneous photocatalytic degradation of phenol on TiO₂/quartz and TiO₂/calcite: A statistical and kinetic approach on comparative efficiencies towards a TiO₂/glass system. *Environ. Sci. Pollut. Res.* **2022**. [[CrossRef](#)]
48. Mino, L.; Zecchina, A.; Martra, G.; Rossi, A.M.; Spoto, G. A surface science approach to TiO₂ P25 photocatalysis: An in situ FTIR study of phenol photodegradation at controlled water coverages from sub-monolayer to multilayer. *Appl. Catal. B Environ.* **2016**, *196*, 135–141. [[CrossRef](#)]
49. Sabzehei, K.; Hadavi, S.H.; Bajestani, M.G.; Sheibani, S. Comparative evaluation of copper oxide nano-photocatalyst characteristics by formation of composite with TiO₂ and ZnO. *Solid State Sci.* **2020**, *107*, 106362. [[CrossRef](#)]
50. Murillo-Acevedo, Y.; Bernal-Sanchez, J.; Giraldo, L.; Sierra-Ramirez, R.; Moreno-Piraján, J.C. Initial Approximation to the Design and Construction of a Photocatalysis Reactor for Phenol Degradation with TiO₂ Nanoparticles. *ACS Omega* **2019**, *4*, 19605–19613. [[CrossRef](#)]
51. Mac Mahon, J.; Pillai, S.C.; Kelly, J.M.; Gill, L.W. Solar photocatalytic disinfection of *E. coli* and bacteriophages MS2, ΦX174 and PR772 using TiO₂, ZnO and ruthenium based complexes in a continuous flow system. *J. Photochem. Photobiol. B Biol.* **2017**, *170*, 79–90. [[CrossRef](#)]
52. Ajona, J.I.; Vidal, A. The use of CPC collectors for detoxification of contaminated water: Design, construction and preliminary results. *Sol. Energy* **2000**, *68*, 109–120. [[CrossRef](#)]

53. Mehrabadi, A.R.; Kardani, N.; Fazeli, M.; Hamidian, L.; Mousavi, A.; Salmani, N. Investigation of water disinfection efficiency using titanium dioxide (TiO₂) in permeable to sunlight tubes. *Desalin. Water Treat.* **2011**, *28*, 17–22. [CrossRef]
54. Alrousan, D.M.A.; Polo-López, M.I.; Dunlop, P.S.M.; Fernández-Ibáñez, P.; Byrne, J.A. Solar photocatalytic disinfection of water with immobilised titanium dioxide in re-circulating flow CPC reactors. *Appl. Catal. B Environ.* **2012**, *128*, 126–134. [CrossRef]
55. Saran, S.; Arunkumar, P.; Devipriya, S.P. Disinfection of roof harvested rainwater for potable purpose using pilot-scale solar photocatalytic fixed bed tubular reactor. *Water Supply* **2018**, *18*, 49–59. [CrossRef]
56. Negishi, N.; Chawengkijwanich, C.; Pimpha, N.; Larpiattaworn, S.; Charinpanitkul, T. Performance verification of the photocatalytic solar water purification system for sterilization using actual drinking water in Thailand. *J. Water Process Eng.* **2019**, *31*, 100835. [CrossRef]
57. Ochoa-Gutiérrez, K.S.; Tabares-Aguilar, E.; Mueses, M.Á.; Machuca-Martínez, F.; Li Puma, G. A Novel Prototype Offset Multi Tubular Photoreactor (OMTP) for solar photocatalytic degradation of water contaminants. *Chem. Eng. J.* **2018**, *341*, 628–638. [CrossRef]
58. Van Der Linde, A.; Tutz, G. On association in regression: The coefficient of determination revisited. *Statistics* **2008**, *42*, 1–24. [CrossRef]
59. Otlávaro-Marín, H.L.; Mueses, M.A.; Crittenden, J.C.; Machuca-Martínez, F. Solar photoreactor design by the photon path length and optimization of the radiant field in a TiO₂-based CPC reactor. *Chem. Eng. J.* **2017**, *315*, 283–295. [CrossRef]
60. Cámara, R.M.; Portela, R.; Gutiérrez-Martín, F.; Sánchez, B. Photocatalytic activity of TiO₂ films prepared by surfactant-mediated sol-gel methods over commercial polymer substrates. *Chem. Eng. J.* **2016**, *283*, 535–543. [CrossRef]
61. Irigoyen-Campuzano, R.; González-Béjar, M.; Pino, E.; Proal-Nájera, J.B.; Pérez-Prieto, J. A Metal-Free, Nonconjugated Polymer for Solar Photocatalysis. *Chem. A Eur. J.* **2017**, *23*, 2867–2876. [CrossRef] [PubMed]
62. Zaruma-Arias, P.E.; Núñez-Núñez, C.M.; González-Burciaga, L.A.; Proal-Nájera, J.B. Solar Heterogeneous Photocatalytic Degradation of Methylthionine Chloride on a Flat Plate Reactor: Effect of pH and H₂O₂ Addition. *Catalysts* **2022**, *12*, 132. [CrossRef]
63. Zhang, Y.; Sivakumar, M.; Yang, S.; Enever, K.; Ramezani-pour, M. Application of solar energy in water treatment processes: A review. *Desalination* **2018**, *428*, 116–145. [CrossRef]
64. Bahnemann, D. Photocatalytic water treatment: Solar energy applications. *Sol. Energy* **2004**, *77*, 445–459. [CrossRef]
65. Hach Company Hach Methods Approved/Accepted by the USEPA. Hach—Downloads—Hach Methods EPA Acceptance Letters. Available online: <https://www.hach.com/cms/documents/pdf/EPA/HachMethodsapprovedacceptedbytheUSEPA.pdf> (accessed on 6 March 2021).
66. Mueses, M.A.; Colina-Márquez, J.; Machuca-Martínez, F.; Li Puma, G. Recent advances on modeling of solar heterogeneous photocatalytic reactors applied for degradation of pharmaceuticals and emerging organic contaminants in water. *Curr. Opin. Green Sustain. Chem.* **2021**, *30*, 100486. [CrossRef]
67. Li, Y.; Yang, B.; Liu, B. MOF assisted synthesis of TiO₂/Au/Fe₂O₃ hybrids with enhanced photocatalytic hydrogen production and simultaneous removal of toxic phenolic compounds. *J. Mol. Liq.* **2021**, *322*, 114815. [CrossRef]
68. Wang, Y.; Zhao, J.; Xiong, X.; Liu, S.; Xu, Y. Role of Ni²⁺ ions in TiO₂ and Pt/TiO₂ photocatalysis for phenol degradation in aqueous suspensions. *Appl. Catal. B Environ.* **2019**, *258*, 117903. [CrossRef]
69. Kuhn, H.; Försterling, H.-D.; Waldeck, D.H. Chemical Kinetics. In *Principles of Physical Chemistry*; John Wiley & Sons, LTD: West Sussex, UK, 2000; pp. 735–794. ISBN 978-0-470-08964-4.
70. Giménez, J.; Curcó, D.; Queral, M. Photocatalytic treatment of phenol and 2,4-dichlorophenol in a solar plant in the way to scaling-up. *Catal. Today* **1999**, *54*, 229–243. [CrossRef]
71. Malato, S.; Fernández-Ibáñez, P.; Maldonado, M.I.; Blanco, J.; Gernjak, W. Decontamination and disinfection of water by solar photocatalysis: Recent overview and trends. *Catal. Today* **2009**, *147*, 1–59. [CrossRef]
72. Ye, J.; Li, X.; Hong, J.; Chen, J.; Fan, Q. Photocatalytic degradation of phenol over ZnO nanosheets immobilized on montmorillonite. *Mater. Sci. Semicond. Process.* **2015**, *39*, 17–22. [CrossRef]
73. Gutiérrez-Alfaro, S.; Acevedo, A.; Rodríguez, J.; Carpio, E.A.; Manzano, M.A. Solar photocatalytic water disinfection of *Escherichia coli*, *Enterococcus spp.* and *Clostridium Perfringens* using different low-cost devices. *J. Chem. Technol. Biotechnol.* **2016**, *91*, 2026–2037. [CrossRef]
74. Pereira, J.H.O.S.; Vilar, V.J.P.; Borges, M.T.; González, O.; Esplugas, S.; Boaventura, R.A.R. Photocatalytic degradation of oxytetracycline using TiO₂ under natural and simulated solar radiation. *Sol. Energy* **2011**, *85*, 2732–2740. [CrossRef]
75. Rincón, A.-G.; Pulgarin, C. Field solar *E. coli* inactivation in the absence and presence of TiO₂: Is UV solar dose an appropriate parameter for standardization of water solar disinfection? *Sol. Energy* **2004**, *77*, 635–648. [CrossRef]
76. Lai, C.-H.; Tang, T. Disaster communication behaviors in the U.S. and China: Which channels do you use and with whom? *J. Appl. Commun. Res.* **2021**, *49*, 207–227. [CrossRef]